Evidence for Anisotropic Coupling between the Protein Environment and the Copper Site in Azurin from Resonance Raman Spectroscopy

M. Adam Webb[†] and Glen R. Loppnow*

Department of Chemistry, University of Alberta, Edmonton, Alberta T6G 2G2, Canada

Received: October 1, 2001; In Final Form: November 29, 2001

A key problem in biological electron transfer is the independent measurement of the parameters upon which the rate constant for electron transfer depends. In this paper, we report evidence that quantitative resonance Raman spectroscopy may be such an independent probe of the electronic coupling parameter in proteins. The resonance Raman cross-sections of four species of azurin have been measured throughout the ca. 600-nm absorption band. The total resonance Raman intensity, as quantified by the cross-sections, is very similar for the four azurins in the 200−700 cm^{-1} region. However, the resonance Raman intensity is distributed differentially among the vibrational modes, sometimes also accompanied by small frequency shifts. Correlations are attempted between this re-distribution of resonance Raman intensity and Cu−S bond length, Cu out-of-plane distance, backbone structure, and protein environment. Of these four parameters, the only significant correlation exists with the protein environment. A detailed analysis of the residues within 10 Å of the copper site demonstrates a strong, anisotropic coupling between the copper site and Trp48, a residue previously implicated in intramolecular electron transfer pathways of azurin.

Introduction

Blue copper proteins, such as azurin, are involved in respiratory and photosynthetic electron transport chains[1−3] and have been used extensively as models for long-range protein electron transfer.[4−16] The active site of azurin is composed of a Cu^{2+} ion strongly coordinated to two histidines and one cysteine, and weakly coordinated to a methionine and the carboxyl oxygen of a glycine.[3] Azurin exhibits a strong absorption band ca. 600 nm that has been assigned as a charge transfer band due to its high oscillator strength, although recent evidence[17,18] suggests the character is more $\pi\pi^*$ and little charge is transferred. Time-resolved absorption spectroscopy of Ru-modified[5−11] or 1-thiouredopyrene-3,6,8-trisulfonic (TUPS) acid-modified[15,16] azurin has shown a dependence of electron transfer rates on protein composition and structure. This dependence has been modeled theoretically as a sequence of through-space, through-bond, and through-hydrogen bond couplings.[5−7] Similar studies on azurin have examined particular electron transfer pathways by combining pulse radiolysis experiments with site-directed mutagenesis of residues between the electron donor and acceptor.[12,13] All of these studies have shown that the molecular nature of the medium is critical for predicting rates of electron transfer.

To understand the molecular mechanism of electron transfer, the roles of distance, medium, orientation, and protein structure must be clearly elucidated. The electron transfer rate constant is dependent on the electronic coupling, H_{DA}, between electron donor and acceptor at the transition state, given by the Marcus equation[19]

$$k = \frac{2\pi}{\hbar}\frac{{H_{DA}}^2}{(4\pi\lambda RT)^{1/2}}e^{-(\Delta G^\circ+\lambda)^2/4\lambda RT} \quad (1)$$

where ΔG° is the standard free energy of reaction and λ is the nuclear reorganization energy. For large separation of donor and acceptor, such as in long-range electron transfer in DNA and proteins, H_{DA} is expected to decay exponentially

$$H_{DA} = H^0_{DA}e^{-\beta(r-r_0)} \quad (2)$$

where H^0_{DA} is the coupling at r_0, r_0 is the van der Waals separation between electron donor and acceptor, r is the actual distance between electron acceptor and donor, and β is an empirical decay constant. A number of both experimental and theoretical studies have suggested that the value of β depends on the particular pathway of the electron transfer[5−7,19] through the intervening medium in large molecules. However, the experimental studies supporting this approach have relied primarily on measurements of the rate constant as a function of distance between donor and acceptor. A recent study[20] has indicated that the parameters upon which the rate constant for electron transfer depends may not be independent; i.e., changing the distance between donor and acceptor may not only affect the coupling but may also affect the reorganization energy and the driving force of the electron transfer reaction.

Resonance Raman spectroscopy may provide information about the electron transfer pathways in proteins and other biological molecules. In resonance Raman spectroscopy, vibrational Raman scattering is excited with radiation at an energy coincident with an electronic transition. The resulting resonance Raman frequencies reflect the normal mode character, while the intensities reflect excited-state structure and dynamics. In proteins, chromophores can be selectively probed by exciting within an absorption band of the chromophore far from any protein absorption. Previous work in our group has extended this idea by varying the protein environment and examining the resulting resonance Raman spectrum of the chromophoric active site, in effect to use the chromophore to project out the important couplings between the active site and protein environment.[21−24]

In this paper, the absorption spectra and quantitative resonance Raman excitation profiles of four azurins from *Pseudomonas*

* To whom correspondence should be addressed. E-mail: glen.loppnow@ualberta.ca.

[†] Current address: Department of Chemistry, University of Idaho, Moscow, ID 83844-2343.

10.1021/jp013665b CCC: $22.00
Published on Web 02/05/2002

aeruginosa (PA), *Alcaligenes denitrificans* (AD), and *Alcaligenes xylosoxidans* (AX I and AX II) have been analyzed. The good correlation of spectral differences with protein composition indicates that resonance Raman spectroscopy is sensitive to the coupling of the copper to the protein environment. Surprisingly, the sensitivity of the resonance Raman spectra appears to be directionally anisotropic; i.e., the spectrum is more sensitive to amino acid changes in some parts of the protein environment than in others. This result suggests an anisotropic long-range coupling between the copper active site and the protein, and that resonance Raman spectroscopy may be sensitive to hard-wired electron transfer pathways important for this protein's function.

Methods

Experimental Details. The two azurins (AX I and AX II) from *A. xylosoxidans* (NCIMB 11015) were isolated and purified from literature procedures[25−27] with slight modifications[24] in the cell rupture and column chromatography steps. Column chromatography was performed using Whatman CM-52 and Sephadex G-50 columns until the purity ratio (A_{280}/A_{620}) was 2.0−4.9 for AX I and 3.1−4.7 for AX II. Typical yields were 4−24 mg of AX I and 4−8 mg of AX II per 100 g of cell paste.

Samples were prepared for resonance Raman experiments by quantitative dilution with a cacodylate buffer solution (0.5−1.0 M cacodylate, 0.01 M TRIS−HCl, pH 8.7). Addition of cacodylate buffer did not have a noticeable effect on the absorption or resonance Raman spectra of azurin. Room-temperature resonance Raman spectra were taken as described previously[21−24,28,29] using 250−300 μL aqueous samples (0.01 M Tris−HCl, pH 8.7, 0.45−0.83 M and 0.34−0.75 M cacodylate for AX I and AX II, respectively) having an absorbance of 1−11 OD/cm and 2−5 OD/cm ca. 620 nm for AX I and AX II, respectively. Bleaching of the sample was accounted for by measuring the absorption at 560 nm ($\epsilon_{560} = 2720$ M^{-1} cm^{-1} for AX I, $\epsilon_{560} = 2710$ M^{-1} cm^{-1} for AX II). For all samples, the overall bleaching was <5%, indicating negligible contributions to the resonance Raman spectrum from photoproducts. The average absorbance was used throughout to calculate the concentration of azurin.

Absolute resonance Raman cross sections of azurin were found using the relative integrated intensities of azurin and cacodylate, as previously described.[21−24,28,29] Absolute Raman cross sections of cacodylate were calculated from the A-term expression.[30] The calculated Raman cross sections for cacodylate are 113, 110, 96.7, 96.0, and 87.1 $\times$ 10^{-14} Å^2/molecule at 579.7, 582.1, 599.6, 600.6, and 613.7 nm, respectively.

Intensity Analysis. The resonance Raman and absorption cross sections in the Condon approximation can be written using the time-dependent equations of Lee and Heller.[31]

$$\sigma_A = \frac{4\pi E_L e^2 M^2}{6\hbar^2 cn}\int_{-\infty}^{\infty} dt\, \langle i|i(t)\rangle \exp\left\{\frac{i(E_L + \epsilon_i)t}{\hbar}\right\} G(t) \quad (3)$$

$$\sigma_R = \frac{8\pi E_S{}^3 E_L e^4 M^4}{9\hbar^6 c^4}\left|\int_{-\infty}^{\infty} dt\, \langle f|i(t)\rangle \exp\left\{\frac{i(E_L + \epsilon_i)t}{\hbar}\right\} G(t)\right|^2 \quad (4)$$

Self-consistent analysis of the absorption spectrum and the resonance Raman excitation profiles was done in the same manner as previously described for plastocyanin[21,22,29] and azurin.[23,24,28] The resonance Raman excitation profiles provided the primary constraints on the simulated spectral band shape and bandwidth. The scaling of the Δ's was determined by the width of the resonance Raman excitation profiles, and the relative Δ's were determined by the relative intensities. The reorganization energy in a mode, λ_i, is related to Δ_i by $\lambda_i = (\Delta_i{}^2\omega_i)/2$, where ω_i is the frequency in cm^{-1}. The total inner-sphere reorganization energy is the sum of the reorganization energy of the individual modes.

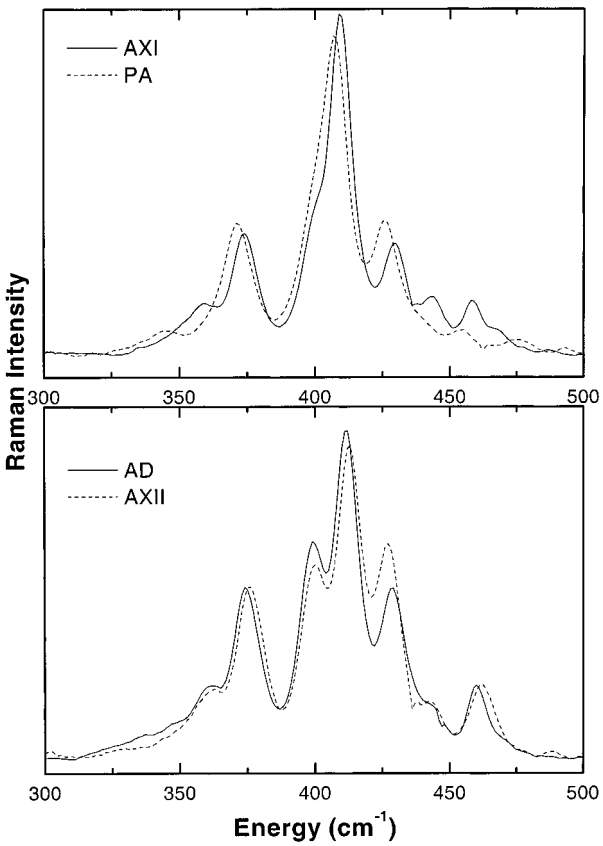

Figure 1. Resonance Raman spectra of azurins from *A. denitrificans* (AD), *A. xylosoxidans* (AX II and AX I), and *P. aeruginosa* (PA) azurin.

Results and Discussion

Analysis of *A. xylosoxidans* I and II. The resonance Raman spectra were taken for the two azurins throughout the 600 nm absorption band. Figure 1 shows the resonance Raman spectra of PA, AD, AX I, and AX II azurins, scaled to the integrated resonance Raman cross-section. Analysis of the quantitative resonance Raman cross-sections of PA and AD azurin have been previously reported.[23,28] Previously[24] it was noted that the spectrum of AX II is comparable to that of AD azurin. Similarly, the resonance Raman spectra of AX I and PA azurin are comparable. Because these pairs also have the smallest sequence variability within 10 Å of the Cu site, these pairs will be used exclusively in the following analysis to ascertain more easily the factors that modulate the resonance Raman intensity. Although comparable, small reproducible differences in frequency and intensity are observed between each member of the pair. These spectral differences were reproducibly observed with the same protein sample, with different protein preparations of the same azurin, and with different excitation wavelengths of the same azurin within the 600 nm absorption band.

The quantitative analysis of these four resonance Raman spectra should yield the structural determinants of excited-state charge transfer in this blue copper protein. Analysis of the

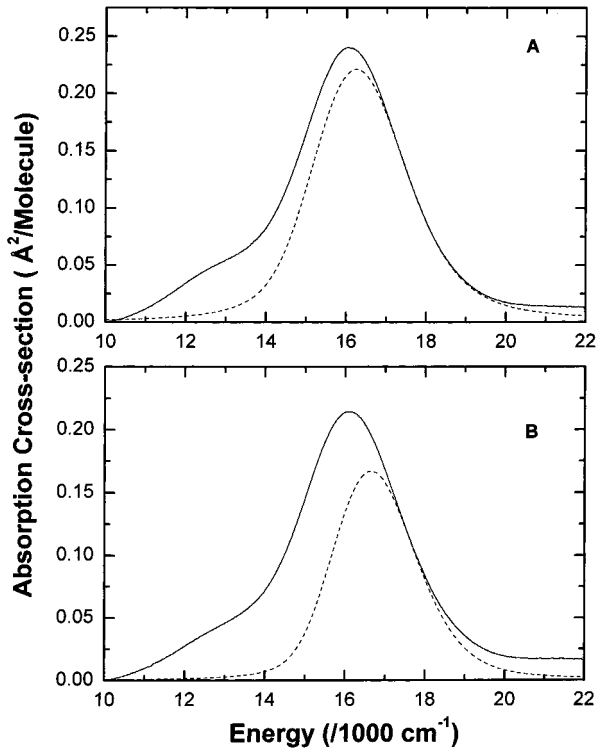

Figure 2. Absorption spectra of *A. xylosoxidans* I/II azurin. (A) Experimental (solid) and calculated (dashed) absorption spectra of *A. xylosoxidans* I azurin. The dashed line was calculated using eq 3 and the parameters in Tables 1 and 2. (B) Experimental (solid) and calculated (dashed) absorption spectra of *A. xylosoxidans* II azurin. The dashed line was calculated using eq 3 and the parameters in Tables 1 and 2.

absorption spectra (Figure 2) and the resulting resonance Raman excitation profiles (Figure 3) with eqs 3 and 4 give the molecular parameters shown in Tables 1 and 2. For the absorption spectrum, the deviations of the fit from the experimental spectrum are due to the presence of electronic transitions, which were not modeled and do not contribute resonance enhancement. To ensure these other transitions do not contribute to the resonance enhancement observed in the 600 nm absorption band,

TABLE 1: Comparison of Mode Frequencies and Displacements for Four Species of Azurin[a]

AD[b]		PA[c]		AX I[d]		AX II[d]	
$\Delta\nu$	$\lvert\Delta\rvert$	$\Delta\nu$	$\lvert\Delta\rvert$	$\Delta\nu$	$\lvert\Delta\rvert$	$\Delta\nu$	$\lvert\Delta\rvert$
212	1.24	216	0.85				
251	0.69	263	1.30	252	0.92	251	0.94
274	1.18			271	0.97	270	0.99
326	0.43						
346	0.93	344	0.75				
360	0.60			360	0.96	362	0.90
375	1.26	371	1.60	374	1.29	376	1.24
399	1.30	401	1.20	398	1.29	399	1.31
412	1.28	408	1.60	410	1.81	413	1.42
428	1.09	426	1.30	429	1.16	426	1.25
443	0.43	439	0.23	444	0.50	440	0.52
460	0.58	454	0.31	458	0.56	462	0.69
		476	0.27	468	0.36		
		493	0.13				
654	0.22	654	0.18				
λ_{tot}	0.25		0.26		0.27		0.24

[a] In this table, $\Delta\nu$ is the vibrational mode frequency in cm^{-1}, Δ is the potential energy curve shift in dimensionless normal coordinates, and λ_{tot} is the total inner-sphere reorganization energy in eV. [b] Values from ref 28. [c] Values from ref 23. [d] Values from this work.

resonance Raman spectra were obtained of azurin at 458 and 700 nm (data not shown). The resulting spectra at these excitation wavelengths were similar to those shown in Figure 1. The resulting molecular parameters can now be compared among all four azurins.

In a previous paper,[24] the resonance Raman spectra were compared to one another in order to test for correlation between spectral intensity differences and structure or sequence. For these comparisons the spectra were normalized to the intensity of the most intense mode. This analysis compared changes of relative intensities and frequencies while ignoring absolute intensity. In this work, the absolute resonance Raman cross sections of both *A. xylosoxidans* azurins have been measured and so the spectra can be scaled to reflect the true cross section. This process will reveal more accurate relationships between the spectroscopic results and molecular structure and composition. The spectra of the four azurins at 568.2 nm were scaled by the Raman cross

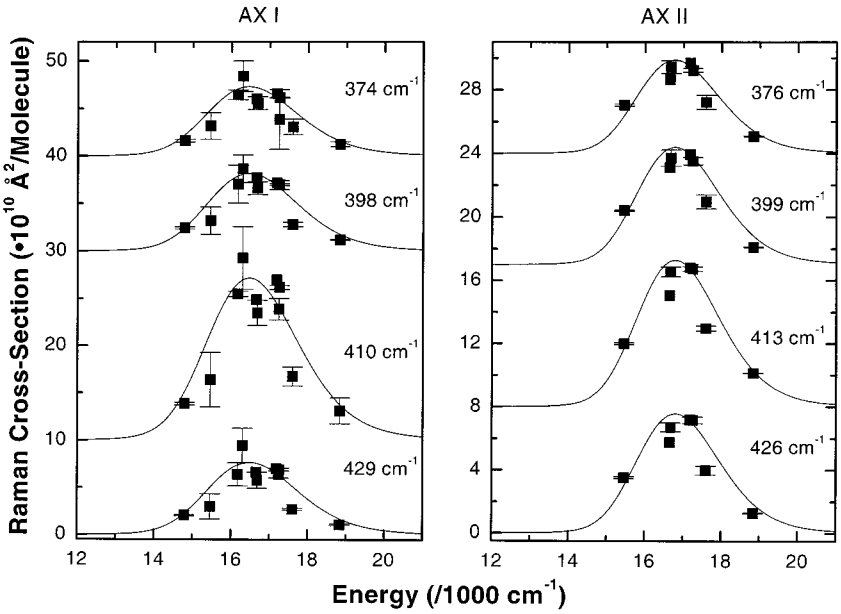

Figure 3. Resonance Raman excitation profiles of azurins I (AX I) and II (AX II) from *A. xylosoxidans* I. The solid lines were calculated using eq 4 with the parameters in Tables 1 and 2.

TABLE 2: Comparison of Excited-state Parameters for Four Species of Azurin[a]

	AD[b]	PA[c]	AX I[d]	AX II[d]
E_0 (cm^{-1})	14 300	14 200	14 150	14 800
M (Å)	0.73	0.63	0.81	0.63
Γ_L (cm^{-1})	450	160	500	285
Γ_G (cm^{-1})	75	0	150	0
θ (cm^{-1})	150	280	0	250
ν_{max} (cm^{-1})	16 150	16 000	16 150	16 100
$\nu_{max,\pi\pi^*}$ (cm^{-1})	16 500	13 600	16 500	16 800
ϵ_{max} ($M^{-1}cm^{-1}$)	52 00	48 00	62 70	57 30
λ_{tot} (eV)	0.25	0.26	0.27	0.24

[a] In this table, E_0 is the zero-zero energy for the resonant state, M is the transition length, Γ_L is the Lorentzian homogeneous line width, Γ_G is the Gaussian homogeneous line width, θ is the inhomogeneous line width, ν_{max} is the maximum of the absorption band, $\nu_{max,\pi\pi^*}$ is the maximum of the simulated $\pi\pi^*$ band, ϵ_{max} is the extinction coefficient at the absorption maximum, and λ_{tot} is the total inner-sphere reorganization energy. Other parameters for the simulation were temperature $T = 0$ K and refractive index $n = 1.33$. [b] Values from ref 28. [c] Values from ref 23. [d] Values from this work.

sections, and the spectral χ^2 values were calculated as before.[24] The χ^2 values are normalized so that the AD/AX II pair gives $\chi^2 = 1.0$. The most similar spectra are AD and AX II ($\chi^2 = 1.0$). The spectrum of PA is most dissimilar with AD and AX II ($\chi^2 = 2.4$ and $\chi^2 = 3.1$) and is closest with AX I ($\chi^2 = 1.2$). AX I is closer to AD than AX II ($\chi^2 = 1.6$ and $\chi^2 = 2.1$). A key result is that the quantitative resonance Raman spectra of the AD/AX II ($\chi^2 = 1.0$) and the PA/AX I ($\chi^2 = 1.2$) pairs exhibit the same magnitude of spectral similarity. Figure 4 shows the correlations of the spectral differences to structure and sequence. The values of RMS difference and % identity are taken from the methods described in the previous paper.[24] The relatively poor correlation of the spectra with structure, as reflected by the RMS difference of the backbone (+0.63) and copper center (−0.43), has not changed significantly. Therefore, the resonance Raman spectra show only a very weak correlation with overall protein structure and no correlation to the copper site geometry. However, the correlation to the Cu−S bond length has increased from 0.41 to 0.64 and suggests a very weak correlation, of similar magnitude as the correlation with the protein backbone. The correlation with % identity increases slightly from −0.88 to −0.91, supporting the hypothesis that the protein environment is the primary influence on the resonance Raman intensities.[24]

Surprisingly, when the four azurin species are compared, an anisotropic response of the resonance Raman spectrum to environment is observed. When PA and AX I azurins are compared, four amino acids (residues 12, 86, 113, and 118) are different within 10 Å of the copper site (Figure 5). Of these four, residues 113 and 118 are directly adjacent to amino acids strongly coordinated to the copper site and are expected to significantly affect the resonance Raman intensities.[21,22] Phe118 is replaced by Ser and Ser113 is replaced by Thr going from PA to AX I. The other two amino acid changes going from PA to AX I are Gly12Gln and Val86Leu, and are not on the same peptide strand as the copper ligands. Gln12 might be expected to have some effect through the introduction of a dipole. The introduction of charges and dipoles have been observed[22] to result in intensity changes of vibrational modes. The Val86Leu change is a conservative substitution and not expected to have an effect on the spectrum. However, in AD and AX II azurin, there is only one amino acid difference within 10 Å of the copper site (Figure 5), the replacement of Trp48 by Leu going from AD to AX II. This one difference appears to have the same effect on the resonance Raman intensities as the four

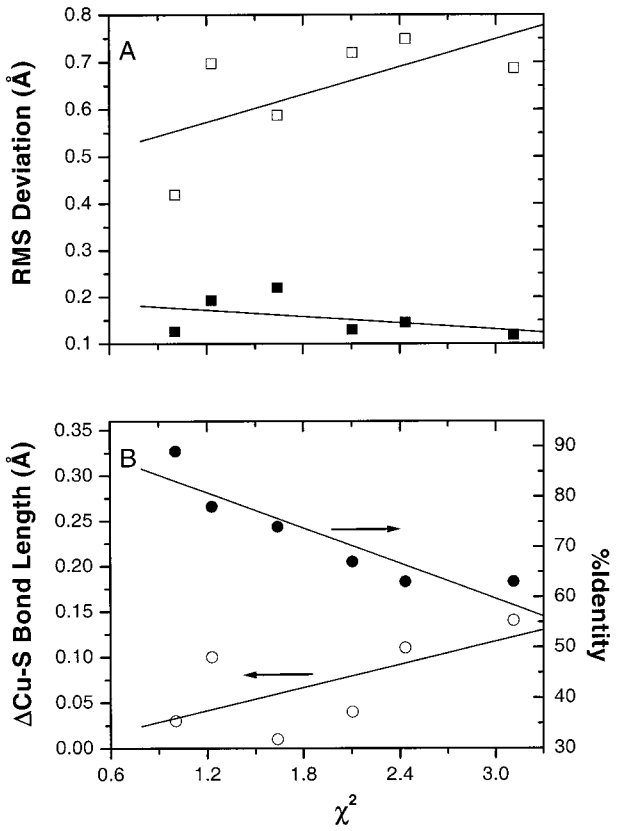

Figure 4. Correlations of the azurin structures and sequences with resonance Raman spectral differences. (A) Correlation of the spectral differences with the RMS deviation of the core atoms ($R = -0.43$, ■) and the protein backbone ($R = 0.63$, □). (B) Correlation of the spectral differences with changes in Cu−S bond length ($R = 0.64$, ○), and % identity ($R = -0.91$, ●). Note that the Raman spectral difference parameter χ^2 is expected to increase as the structural difference parameters, RMS deviation and ΔCu−S bond length, increase. However, χ^2 is expected to *decrease* as the % identity increases, as the % identity is a measure of environmental similarity.

changes in the PA/AX I pair. This is a significant change in side-chain properties only three amino acids from the copper site along a peptide strand from the strongly coordinated His46. For plastocyanin,[22] it was found that changes in amino acids that are within 2−3 amino acids of the copper ligands along the same peptide strand can significantly affect the distribution of intensity of the observed normal modes, perhaps because the normal modes of the Cu site chromophore are actually delocalized into the protein backbone via the coordinating amino acids. This apparent anisotropic coupling between the copper chromophore and the protein environment is discussed in more detail below in relation to the electron transport properties of this protein.

Molecular Parameters. The absorption spectra and the resulting resonance Raman excitation profiles have been quantitatively analyzed for four azurin species. A full analysis, as performed here, is needed to obtain accurate results in cases where the assumptions sometimes used to simplify the calculation fail. For example, some methods for calculating reorganization energy make the assumption that the absorption bandwidth is determined solely by the Franck−Condon vibronic progression in the resonance Raman active modes. This has not been the case for azurin and plastocyanin.[21−24,28,29] It was found that the intense $\pi\pi^*$ transition does not correspond to the absorption maximum as might be expected and that there was a significant contribution to the absorption spectrum by other electronic transitions.

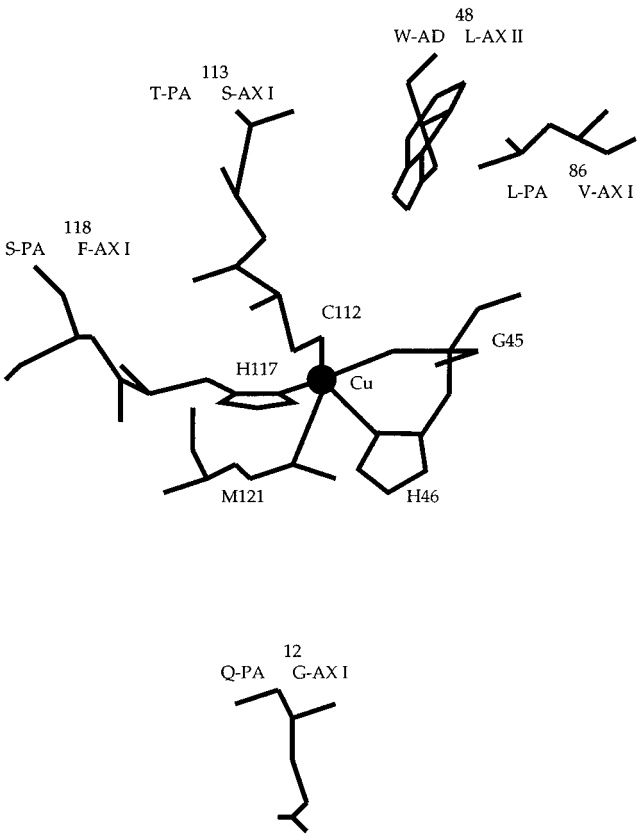

Figure 5. Partial structure of *P. aeruginosa* azurin near the copper site, after Nar et al.[35] One-letter codes are shown for the amino acids that differ between the AD/AX II and AX I/PA pairs of azurins within 10 Å of the copper site. Also shown is the copper ion and the five nominal copper ligands.

Self-consistent analysis of the absorption spectrum and the resulting resonance Raman excitation profiles of four azurins gives a number of molecular parameters, compared in Tables 1 and 2. Although the absorption spectra are similar among the four azurins, variations in ν_{max} and ϵ_{max} are observed and may be consistent with small changes in the electronic structure. Changes in amino acids (i.e., charges/dipoles) and in structure around the copper may result in perturbations to the electronic structure. The similarity of the absorption spectra may be due to the highly conserved nature of the copper metal site. Although the overall absorption spectrum changes with species, the calculated $\pi\pi^*$ energies, measured at the maximum of the simulated electronic transition, from the resonance Raman excitation profiles are more similar among the species (Table 2) and are likely a result of the highly conserved nature of the copper active site.

Parameters such as the transition length (*M*) and partitioning of the broadening into homogeneous and inhomogeneous components vary significantly between species and do not follow any easily discernible pattern. There are two possible reasons for the seemingly random parameters between species. The first is that the observed differences are related in a complex manner to the properties of the azurin species. The amino acid sequences and geometry are different for each species, reflecting the separate evolution of each species. A second possibility is that the analysis described here does not yield unique answers. A significant limitation on the restraint of the parameters is the complexity of the absorption spectrum. It is known that there are other transitions in this region, with the band at ~620 nm being assigned to the $\pi\pi^*$ absorption transition. Solomon and co-workers[32] locate the $\pi\pi^*$ band of *P. aeruginosa* at 16 220 cm^{-1}, which compares well with a value of 16 300 cm^{-1} obtained from resonance Raman spectroscopy[28] and Stark spectroscopy.[18] The similarity of the electronic properties from these three different methods suggests that the parameters here are robust. However, dynamic or low-temperature trapped hole-burning studies may provide further evidence for whether the observed differences in homogeneous and inhomogeneous broadening among the four azurins are environmentally dependent.

Electron Transfer. One goal of this work is to tie the results we have obtained to the electron transfer function of azurin. At first glance, it is not obvious why resonance Raman spectroscopy of this $\pi\pi^*$ transition should be relevant for understanding thermal, nonphotochemical electron transfer in these proteins. Although the frequencies reflect the ground-state normal mode character, the intensities reflect excited-state properties, one of which may be Duschinsky rotation, different normal modes in the excited-state as a result of the altered electronic structure. Past studies, however, have shown that Duschinsky rotation in both the azurins and plastocyanins is negligible.[23,28] Therefore, our strategy of using the chromophoric Cu site to project out certain active site vibrations and examining how they are modulated by the protein environment is reflecting the ground-state normal modes, a subset of which are important for the physiologically relevant electron transfer. Previous studies[10,33] have shown that the Cu site $\pi\pi^*$ absorption transition is strongly coupled to the electron transfer and could provide a good model for understanding the electron transfer pathway. Thus, the resonance-enhanced normal modes observed here may be significant in the electron transfer pathway. Electron transfer studies[4,10,16] measuring electron transfer rates through different pathways have found more efficient coupling through Cys112 than the other coordinating ligands, which suggests that the protein may have preferred pathways for electron transfer.

The rate of electron transfer, *k*, is related to the standard free energy of reaction, $\Delta G°$, and the nuclear reorganization energy, λ as shown in eq 1[2]. Electrons are thought to pass through Cys112,[4] and the reorganization energy of the 600 nm absorption band may be a contribution to the inner-sphere reorganization energy of electron transfer. In previous papers,[23,28] the total inner-sphere reorganization energy for this excited state was measured for PA and AD azurin (Table 1). The total reorganization energies determined here for AX I and II azurins are similar to those (0.255 ± 0.012 eV) and may show how these proteins have similar properties in order to serve similar functions in each species. The sum of the experimental cross sections are also very similar for the four azurins. Since the total reorganization energy is proportional to the sum of the intensity, it would be expected that the total reorganization energy would be similar. However, the distribution of reorganization energy among the vibrational modes is different among the species due to variations in the amino acids that alter the environment of the copper metal ion (vida supra), and it is this fact that suggests the resonance Raman spectrum may be reflecting these electron transfer pathways in the protein.

Intramolecular electron transfer has been studied extensively with azurin, because the disulfide bridge provides a convenient source of an electron and the electron transfer can be easily triggered photolytically.[12] Theoretically, two electron transfer routes have been calculated to model the experimental electron transfer between Cys3 of the disulfide bridge and the copper site.[4] These two routes are shown in Schemes 1 and 2, where ts and tb correspond to through-space and through-bond jumps, respectively. In Scheme 1, one route starts with a through-space

SCHEME 1

$$\text{Cys3} \xrightarrow{ts} \text{Thr30} \xrightarrow{tb} \text{Val31} \xrightarrow{ts} \text{Trp48} \xrightarrow{tb} \text{Val49} \xrightarrow{ts} \text{Phe1111} \xrightarrow{tb} \text{Cys112} \xrightarrow{tb} \text{Cu}$$

SCHEME 2

$$\text{Cys3} \xrightarrow{tb} \text{Ser4} \xrightarrow{tb} \text{Val5} \xrightarrow{tb} \text{Asp6} \xrightarrow{tb} \text{Ile7} \xrightarrow{tb} \text{Gln8} \xrightarrow{tb} \text{Gly9} \xrightarrow{tb} \text{Asn10} \xrightarrow{ts} \text{His46} \xrightarrow{tb} \text{Cu}$$

jump from Cys3 to Thr30. The electron goes to Val31 and a second through-space jump to Trp48. The electron continues through Val49 and a third through-space jump to Phe111. The electron passes through Cys112 and finally reaches the copper. In Scheme 2, the other pathway follows the peptide chain from Cys3 to Asn10 before a through-space jump to His46 and then to the copper. Note that of the amino acid changes in the different species, only Trp48 forms part of these electron transfer paths.

An intriguing interpretation of the anisotropic effect of amino acid composition on the resonance Raman spectra is that the spectra are sensitive to long-range vibrational mixing, probably because the Cu site normal modes are delocalized somewhat into the protein backbone and, thus, may reflect the vibrational coordinates for electron transfer through the protein. The amino acid sequence and structure of the protein is thought to be related to the electron transfer function of the protein. Research has shown that the electron transfer properties of PA azurin depend[5,6,10,11] on the composition and secondary structure of the protein along the electron transfer pathway. In the simplest description of long-range electron transfer, the electron transfer rate decays exponentially with distance, modulated by some distance-decay constant. The predicted distance-decay constants are 1.26 $Å^{-1}$ for an α-helix and 1.00 $Å^{-1}$ for a β-strand.[5,6] The intramolecular electron transfer rates of five Ru-modified derivatives of azurin were measured,[5,6] giving a decay constant for azurin of 1.10 $Å^{-1}$, which is close to the predicted value for the β-strand and consistent with the secondary structure of azurin. The electron transfer rate may also be affected by the properties of specific amino acids, but this has been controversial. Calculations using a tight-binding extended Hückel type method show that the aromatic amino acid side chains do not promote electron transfer.[34] However, experimental measurements of intramolecular electron transfer of *P. aeruginosa* mutants show significant rate changes in some Trp48 mutants[4]—changing Trp48 to Phe or Try increases the electron transfer rate constant, k_{ET}, from 44 to 80 and 85 s^{-1}, respectively. Amino acids such as Ala and Met decrease the rate slightly ($k_{ET} = 35$ and 33 s^{-1}, respectively), while Ser slightly increases the electron transfer rate ($k_{ET} = 50$ s^{-1}).[4] Interestingly, mutation of Val31 to Trp increases the rate almost 7-fold, presumably due to π-stacking interactions with Trp48 that facilitate electron transfer. These results are consistent with the significant effect this residue has on the resonance Raman spectra, and suggests the resonance Raman spectrum may be a uniquely sensitive probe of electron transfer pathways in these proteins. However, when Trp48 is replaced with Leu in PA, analogous to the change in AD/AX II azurin, the intramolecular electron transfer rate is not significantly affected.[4] This suggests that the electronic coupling has not changed and the resonance Raman spectrum may reflect changes in vibrational properties alone, which may or may not be important in the physiological electron transport function of this protein. The conflicting evidence makes the contextual interpretation of the resonance Raman spectroscopy difficult. Clearly, concurrent measurement of electron transfer rates and resonance Raman spectra for particular mutants of azurin should clarify the relationship between amino acid composition, electron transfer kinetics, and the resonance Raman spectra.

Conclusion

The absorption spectra and resonance Raman excitation profiles have been analyzed for four species of azurin. The total inner-sphere reorganization energy was found to be the same for the four species. This may be related to the function of the protein, with the low value facilitating rapid electron transfer. It was found that although there is a very weak correlation of spectral differences with protein structure, the primary influence on the resonance Raman spectra appears to be the protein environment. Anisotropic coupling was observed with extended vibrational mixing along a proposed electron transfer route. The results are consistent with greater coupling of the copper through Cys112, suggesting that resonance Raman may be sensitive to the parameters and pathways of long-range intramolecular electron transfer.

Acknowledgment. We thank R. Mah and M. Pickard at the University of Alberta for the growth and harvesting of *A. xylosoxidans*. Financial support for this work was provided by NSERC Canada through the Research Grants-in-aid Program.

Supporting Information Available: Figures 1S and 2S showing the resonance Raman spectra of *A. xylosoxidans* azurin I and II, respectively, as a function of excitation wavelength, and Tables 1S and 2S listing the experimental and calculated Raman cross-sections for *A. xylosoxidans* azurin I and II as a function of excitation wavelength and mode frequency. This material is available free of charge via the Internet at http://pubs.acs.org.

References and Notes

(1) Adman, E. T. *Adv. Protein Chem.* **1991**, *42*, 145.
(2) Sykes, A. G. *Inorg. Chem.* **1991**, *36*, 377.
(3) Adman, E. T. In *Metalloproteins-Part I: metal Proteins with Redox Roles*; Harrison, P. M., Ed.; Verlag Chemie: Deerfield Beach, FL, 1985; p 1.
(4) Farver, O.; Skov, L. K.; Young, S.; Bonander, N.; Karlsson, G. B.; Vanngard, T.; Pecht, I. *J. Am. Chem. Soc.* **1997**, *119*, 5453.
(5) Gray, H. B.; Winkler, J. R. *Annu. Rev. Biochem.* **1996**, *65*, 537.
(6) Langen, R.; Chang, I.-J.; Germanas, J. P.; Richards, J. H.; Winkler, J. R.; Gray, H. B. *Science* **1995**, *268*, 1733.
(7) Gray, H. B.; Winkler, J. R. *J. Electroanal. Chem.* **1997**, *438*, 43.
(8) Margalit, R.; Kostic, N. M.; Che, C.-M.; Blair, D. F.; Chiang, H.-J.; Pecht, I.; Shelton, J. B.; Shelton, J. R.; Schroeder, W. A.; Gray, H. B. *Proc. Natl. Acad. Sci. U.S.A.* **1984**, *81*, 6554.
(9) Bjerrum, M. J.; Casimiro, D. R.; Chang, I.-J.; Di Bilio, A. J.; Gray, H. B.; Hill, M. G.; Langen, R.; Mines, G. A.; Skov, L. K.; Winkler, J. R.; Wuttke, D. S. *J. Bioenerg. Biomem.* **1995**, *27*, 295.
(10) Regen, J. J.; Di Bilio, A. J.; Winkler, J. R.; Richards, J. H.; Gray, H. B. *Inorg. Chim. Acta* **1998**, *275*−*6*, 470.
(11) Skov, L. K.; Pascher, T.; Winkler, J. R.; Gray, H. B. *J. Am. Chem. Soc.* **1998**, *120*, 1102.
(12) Farver, O.; Pecht, I. *Proc. Natl. Acad. Sci. U.S.A.* **1989**, *86*, 6968.
(13) Farver, O.; Pecht, I. *J. Am. Chem. Soc.* **1992**, *114*, 5764.
(14) Farver, O.; Skov, L. K.; Gilardi, G.; van Pouderoyen, G.; Canters, G. W.; Wherland, S.; Pecht, I. *Chem. Phys.* **1996**, *204*, 271.
(15) Kotlyar, A. B.; Borovok, N.; Hazani, M. *Biochemistry* **1997**, *36*, 15828.
(16) Borovok, N.; Kotlyar, A. B.; Pecht, I.; Skov, L. K.; Farver, O. *FEBS Lett.* **1999**, *457*, 277.
(17) Solomon, E. I.; Lowery, M. D. *Science* **1993**, *259*, 1575.
(18) Chowdhury, A.; Peteanu, L. A.; Webb, M. A.; Loppnow, G. R. *J. Phys. Chem. B* **2001**, *105*, 527.

(19) Marcus, R. A.; Sutin, N. *Biochim. Biophys. Acta* **1985**, *811*, 265.
(20) Kelley, S. O.; Barton, J. K. *Science* **1999**, *283*, 375.
(21) Loppnow, G. R.; Fraga, E. *J. Am. Chem. Soc.* **1997**, *119*, 896.
(22) Fraga, E.; Loppnow, G. R. *J. Phys. Chem. B* **1998**, *102*, 7659.
(23) Webb, M. A.; Loppnow, G. R. *J. Phys. Chem. B* **1998**, *102*, 8923.
(24) Webb, M. A.; Loppnow, G. R. *J. Phys. Chem. A* **1999**, *103*, 6283.
(25) Ambler, R. P. *Biochem. J.* **1963**, *89*, 341.
(26) Abraham, Z. H. L.; Lowe, D. J.; Smith, B. E. *Biochem. J.* **1993**, *295*, 587.
(27) Dodd, F. E.; Hasnain, S. S.; Hunter, W. N.; Abraham, Z. H. L.; Debenham, M.; Kanzler, H.; Eldridge, M.; Eady, R. R.; Ambler, R. P.; Smith, B. E. *Biochemistry* **1995**, *34*, 10180.
(28) Webb, M. A.; Kwong, C. M.; Loppnow, G. R. *J. Phys. Chem. B* **1997**, *101*, 5062.
(29) Fraga, E.; Webb, M. A.; Loppnow, G. R. *J. Phys. Chem.* **1996**, *100*, 3278.
(30) Albrecht, A. C.; Hutley, M. C. *J. Chem. Phys.* **1971**, *55*, 4438.
(31) Lee, S.-Y.; Heller, E. J. *J. Chem. Phys.* **1979**, *71*, 4777.
(32) Solomon, E. I.; Hare, J. W.; Dooley, D. M.; Dawson, J. H.; Stephens, P. J.; Gray, H. B. *J. Am. Chem. Soc.* **1980**, *102*, 168.
(33) Dong, S.; Spiro, T. G. *J. Am. Chem. Soc.* **1998**, *120*, 10434.
(34) Broo, A.; Larsson, S. *J. Phys. Chem.* **1991**, *95*, 4925.
(35) Nar, H.; Messerschmidt, A.; Huber, R.; van de Kamp, M.; Canters, G. W. *J. Mol. Biol.* **1991**, *221*, 765.